Let-7a Down-Regulation Plays a Role in Thyroid Neoplasias of Follicular Histotype Affecting Cell Adhesion and Migration through Its Ability to Target the *FXYD5* (Dysadherin) Gene

Marianna Colamaio, Gaetano Calì, Daniela Sarnataro, Eleonora Borbone, Pierlorenzo Pallante, Myriam Decaussin-Petrucci, Lucio Nitsch, Carlo Maria Croce, Sabrina Battista, and Alfredo Fusco

Istituto di Endocrinologia ed Oncologia Sperimentale del Consiglio Nazionale delle Ricerche c/o Dipartimento di Biologia e Patologia Cellulare e Molecolare (M.C., G.C., E.B., P.P., L.N., S.B., A.F.), Facoltà di Medicina e Chirurgia di Napoli, Università degli Studi di Napoli "Federico II", 80131 Napoli, Italy; CEINGE Biotecnologie Avanzate (M.C., D.S., E.B., P.P., L.N., S.B., A.F.), 80131 Napoli, Italy; Department of Pathology (M.D.-P.), Centre Hospitalier Lyon-Sud, Hospices Civils de Lyon, Université Lyon 1, 69495 Pierre Bénite, France; and Department of Molecular Virology, Immunology, and Medical Genetics (C.M.C.), Comprehensive Cancer Center, Ohio State University, Columbus, Ohio 43210

Context: Thyroid neoplasias of the follicular histotype include the benign follicular adenomas and the malignant follicular carcinomas. Although several genetic lesions have already been described in human thyroid follicular neoplasias, the mechanisms underlying their development are still far from being completely elucidated. MicroRNAs (miRs or miRNAs) have recently emerged as important regulators of gene expression, also playing a key role in the process of carcinogenesis.

Objective: The aim of our work has been to identify the miRNAs differentially expressed in human thyroid follicular neoplasias and define their role in thyroid carcinogenesis.

Design: The miRNA expression profile of 10 human thyroid follicular adenomas was compared to that of 10 normal thyroid tissues.

Results: The miRNA expression profiles revealed the down-regulation of let-7a in thyroid follicular adenomas compared to normal thyroid. Then, quantitative RT-PCR analyses validated the microarray data and showed a significantly higher decrease in let-7a expression in follicular carcinomas. Enforced let-7a expression in the follicular thyroid carcinoma cell line WRO induces an epithelial-like phenotype, increases cell adhesion, and decreases cell migration. Conversely, silencing of let-7a in the normal rat thyroid cell line PC Cl 3 has opposite effects. We identified dysadherin (FXYD5), a cell membrane glycoprotein, correlated with tumor progression and invasiveness, as a target of let-7a. Consistently, an inverse correlation between dysadherin and let-7a expression levels was found in human thyroid follicular adenomas and carcinomas.

Conclusions: These results suggest a role of let-7a down-regulation in the development of thyroid neoplasias of the follicular histotype, likely regulating dysadherin protein expression levels. **(*J Clin Endocrinol Metab* 97: E2168–E2178, 2012)**

Human thyroid neoplasias include benign and malignant tumors. Most thyroid cancers are derived from the follicular cell and include differentiated and undifferentiated histotypes. Differentiated thyroid carcinomas include papillary (PTC) and follicular histotypes (adenomas and carcinomas, abbreviated FA and FTC, respectively), and in most of

ISSN Print 0021-972X ISSN Online 1945-7197
Printed in U.S.A.

doi: 10.1210/jc.2012-1929 Received April 10, 2012. Accepted August 21, 2012.
First Published Online September 10, 2012

Abbreviations: EMT, Epithelial-mesenchymal transition; FA, follicular adenoma; FN, fibronectin; FTC, follicular thyroid carcinoma; GAPDH, glyceraldehyde-3-phosphate dehydrogenase; miRNA, microRNA; PTC, papillary thyroid carcinoma; qRT-PCR, quantitative RT-PCR; UTR, untranslated region; VN, vitronectin.

the cases they have a good prognosis (1). Conversely, anaplastic thyroid cancer is one of the most lethal human cancers. FA is a common benign tumor that presents as a solitary nodule, usually as a painless mass, and may be found during a routine physical examination. Adenomas of this class are usually nonfunctioning (cold at scintigraphy), whereas few are hyperfunctioning toxic adenomas (hot on scintigraphy). Preoperative cytological analyses do not allow the distinction between FA and FTC, which is possible only after surgical intervention by the careful examination of the capsule, whose invasion represents the hallmark of malignancy (2). At odds with PTCs, FTCs frequently manifest vascular invasion with the presence of metastases at the lungs and bones (1). Molecular studies have in part identified the molecular mechanisms leading to thyroid cancer initiation and progression. Somatic mutations in the TSH receptor (*TSHR*) gene, and less frequently in the adenylate cyclase-stimulating G α protein (GNAS), have been found in toxic adenomas (3). Conversely, point mutations of the *ras* gene family and the t(2;3)(q13;p25) translocation, resulting in the fusion of *PAX8* and peroxisome proliferator-activated receptor γ (*PPAR*γ) (4), are present in nontoxic adenomas and FTCs. Variants of Forkhead box E1 (*FOXE1*) (or thyroid transcription factor 2, *TTF2*) and NK2 homeobox 1 (*NKX2-1*) (also known as thyroid transcription factor 1, *TTF1*) account for an increased risk of both PTC and FTC (5). However, although several genetic lesions have been described already in human thyroid follicular neoplasias, the mechanisms underlying their development are still far from being completely elucidated. MicroRNAs (miRNAs) are important regulators of gene expression that play key roles in the process of carcinogenesis (6). Previous studies showed an aberrant miRNA expression profile that distinguishes unequivocally among PTCs, anaplastic thyroid cancers, and normal thyroid tissue (7, 8). Conversely, relatively little is known about miRNAs differentially expressed in FAs and FTCs. Therefore, in this study, we have analyzed the miRNA expression profile of 10 FA samples *vs.* 10 normal thyroid tissues. A subset of miRNAs was found to be down-regulated in FA. Among these miRNAs, we focused on let-7a belonging to the let-7 family of miRNAs. This family includes 13 members (*let-7a-1*, *7a-2*, *7a-3*, *7b*, *7c*, *7d*, *7e*, *7f-1*, *7f-2*, *7g*, *7i*, *mir-98*, and *miR-202*) (9), widely considered tumor suppressor genes because their expression is lost in many cancers, such as lung (10), breast (11), and gastric carcinomas (12), and the exogenous delivery of let-7 prevents the formation of lung tumors from premalignant lesions and shrinks tumors carrying activating *RAS* mutations (13). Consistent with the antioncogenic role of the let-7 family members, *RAS* (14), *HMGA2* (15), *c-MYC* (16), *cyclins B1*, *E2*, *F*, *G2*, and *CDC2*, *25*, and *34* (17) have been identified as their targets. The results reported here suggest a role of let-7a down-regulation in the process that leads to follicular thyroid neoplasias. Indeed, we show that enforced expression of let-7a in the FTC cell line WRO affects cell morphology leading to an epithelial-like morphology, increases cell adhesion, and decreases cell migration, whereas the let-7a silencing in normal rat thyroid cells has opposite effects. Finally, we identify dysadherin (FXYD5) as one of the let-7a targets, likely partially accounting for the effects exerted by let-7a on cell morphology, adhesion, and migration.

Materials and Methods

Thyroid tissue samples

Human neoplastic thyroid tissues and normal adjacent tissue or the contralateral normal thyroid lobe of patients with nontoxic FA and FTC were obtained from surgical specimens collected at the Service d'Anatomo-Pathologie, Centre Hospitalier (Lyon Sud, Pierre Benite, France) and immediately frozen in liquid nitrogen. The tumor samples were stored frozen until RNA or protein extractions were performed, after pulverizing the tumors by using dry ice-chilled stainless steel mortar and pestles. All thyroid tissue diagnoses were confirmed histologically. Informed consent was obtained for scientific use of biological material from all patients.

miRNACHIP microarray

Microarray experimental procedures were performed as previously described (7).

RNA extraction and quantitative RT-PCR (qRT-PCR)

RNA extraction and qRT-PCR were performed as described (18). Primers (miScript Primer Assay; QIAGEN, Hilden, Germany) were: Hs_let-7a_1 (amplifying human and rat let-7a) and Hs_RNU6B_2 (amplifying human and rat U6), used as loading control. For *FXYD5* mRNA detection, total RNA was reverse transcribed from tumor samples and cell lines by using the QuantiTect Reverse Transcription Kit (QIAGEN), and qRT-PCR was performed by using Power SYBR Green PCR Master Mix (Applied Biosystems, Foster City, CA). *G6PD* was used as loading control. Primer sequences are specified in Supplemental Materials and Methods (published on The Endocrine Society's Journals Online web site at http://jcem.endojournals.org). The $2^{-\Delta\Delta Ct}$ formula was used to calculate the differential gene expression.

Cell cultures and stable transfections

The human WRO cell line from FTC, the normal and transformed rat thyroid cell lines, and their culture conditions have been described elsewhere (19, 20). For stable transfections of WRO and PC Cl 3 cells, Arrest-in Transfection reagent (Open Biosystems, Huntsville, AL) was used, following the manufacturer's instructions. Five $\times$ 10^5 cells were plated in 100-mm dishes, and 4 μg of the Hsa-let-7a expressing or silencing constructs (see Supplemental Materials and Methods) or the respective empty vectors were transfected. Forty-eight hours after transfection, cells were selected with 0.5 μg/ml puromycin.

TSH induction

TSH induction is described in Supplemental Materials and Methods.

Plasmids

Plasmids are described in Supplemental Materials and Methods.

Cell migration assays

Wound-induced migration and transwell assays are described in Supplemental Materials and Methods.

Protein extraction, Western blotting, and antibodies

Total proteins extraction and Western blotting were performed as in Pallante *et al.* (21).

Primary antibodies used were anti-HMGA2 (22) antihuman FXYD5 monoclonal antibody (M53) (23), kindly donated by Dr. Setsuo Hirohashi (Pathology Division, National Cancer Center Research Institute, Tokyo, Japan); antirat FXYD5 (R-15) (Santa Cruz Biotechnology, Santa Cruz, CA); anti-glyceraldehyde-3-phosphate dehydrogenase (GAPDH) (Santa Cruz Biotechnology); and anti-α-tubulin (Sigma-Aldrich, St. Louis, MO). Blots were visualized by using the Western blotting detection reagents (GE Healthcare, Buckinghamshire, UK).

Immunofluorescence and confocal microscopy

Immunofluorescence and confocal microscopy are described in Supplemental Materials and Methods.

Adhesion assay

Cell adhesion assays were performed as described (24). Ninety-six-well plates were incubated overnight with fibronectin (FN) (10 μg/ml), or vitronectin (VN) (10 μg/ml), both from Sigma-Aldrich, or 1% BSA in PBS. Attached cells were stained with crystal violet 0.5% and washed in PBS, and the plates were read at 570 nm in a microplate reader (LX 800, Universal Microplate Reader; BioTek, Winooski, VT).

Dual-luciferase reporter assay

Dual-luciferase reporter assay is described in Supplemental Materials and Methods.

Statistical analysis

Data are presented as mean ± SD. Statistical significance of the differences in experimental data were analyzed by Student's *t* test ($P < 0.05$ was regarded as significant).

Results

Let-7a is down-regulated in FAs and FTCs

We used a miRNA CHIP microarray (25) to evaluate the miRNA expression profile of 10 nontoxic FAs and 10 normal thyroid tissues. The neoplastic samples were all matched with their corresponding normal thyroid tissues. By applying ANOVA analysis, we obtained a list of differentially expressed miRNAs ($P < 0.05$) between normal and neoplastic thyroids (Supplemental Table 1). Among the miRNAs down-regulated in FAs with respect to normal thyroid, we identified several miRNAs of the let-7 family. Then, we focused our attention on these miRNAs because previous studies have identified them as tumor suppressor genes (10–13). The microarray data were validated by quantitative stem-loop RT-PCR in a larger panel of FA and FTC samples. As shown in Fig. 1A, let-7a was down-regulated in FAs (average fold change, 4.16) and FTCs (average fold change, 8.33) (Fig. 1B) in comparison with normal thyroid. The box plot analysis of let-7a expression in FAs and FTCs (Fig. 1C) allows us to estimate the average let-7a expression level in FTCs as significantly lower compared with FAs ($P = 0.0041$). Therefore, the down-regulation of let-7a in both FAs and FTCs suggests that this may be an early event in the process of carcinogenesis of follicular tumors.

Let-7a is down-regulated in transformed rat thyroid cells

The analysis of let-7a expression in rat thyroid cells, PC Cl 3, transformed by the oncogenes v-*mos*, v-*raf*, and v-*ras-Ha* shows a reduced let-7a expression in the transformed cells in comparison to the normal ones (Fig. 1D), suggesting that let-7a down-regulation may be a general event in thyroid cell transformation. Interestingly, we observed down-regulation of let-7a expression in PC Cl 3 cells stimulated to proliferate after treatment with TSH (Fig. 1E). This result would confirm the association of let-7a down-regulation with thyroid cell growth, strengthening the hypothesis of a tumor suppressor role of let-7a in thyroid carcinogenesis.

Overexpression of let-7a in WRO thyroid cells induces an "epithelial" phenotype

To define the role of let-7a down-regulation in thyroid carcinogenesis, we restored its expression in a human FTC cell line, WRO, that shows a reduced let-7a expression in comparison with normal thyroid (Fig. 2A, *left panel*). We transfected WRO cells with a U6-driven let-7a expressing vector (see *Materials and Methods*) carrying a puromycin-resistance gene. As shown in Fig. 2A (*right panel*), the selected puromycin-resistant cell clones (WROlet-7a) express higher levels of let-7a compared with clones transfected with the empty vector (WROhU6). Consistently, WROlet-7a cells show lower levels of the HMGA2 and RAS proteins (Fig. 2B and data not shown, respectively), two previously identified let-7 targets (14, 15), in comparison with WROhU6 cells. WROlet-7a cell clones show enlarged, flattened, polygonal, and more adherent-looking morphology, compared with WROhU6 cells (Fig. 2C). Immunofluorescence with phalloidin and anti-α-tubulin

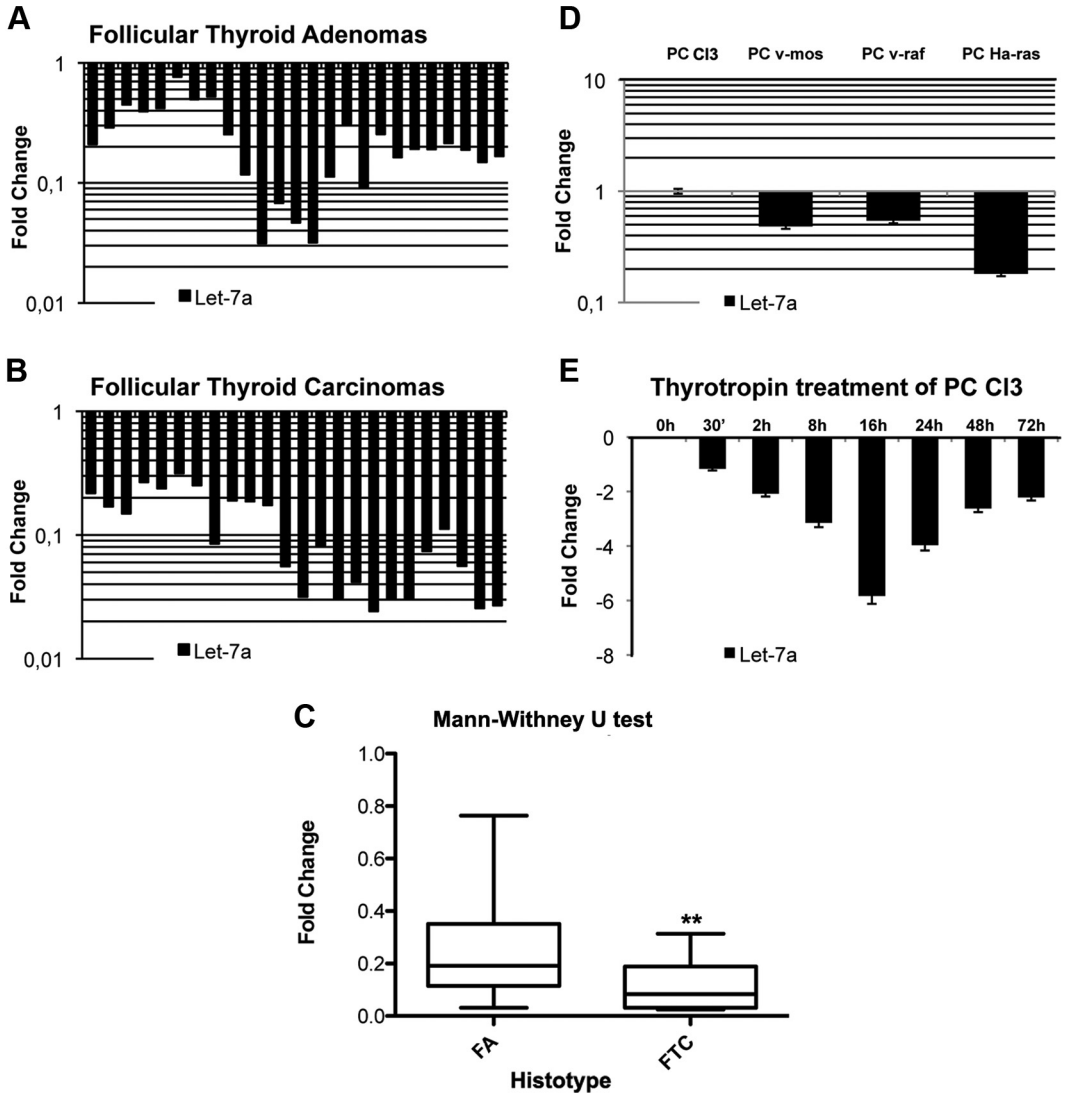

FIG. 1. Let-7a expression in thyroid tumors and cell lines. Analysis of let-7a expression by qRT-PCR. Let-7a expression in a panel of thyroid FAs (n = 25) compared with normal thyroid (A), FTCs (n = 24) compared with normal thyroid (B), and box plot analyses of let-7a expression in the same tumors (Mann-Whitney *U* test) (C). *Asterisks* indicate the significance of the difference in let-7a expression between FAs and FTCs ($P = 0.0041$). The fold change values indicate the relative change in the expression levels between tumor samples and the mean of three reference thyroids (A and B, normal thyroids), assuming the latter to be equal to 1. The range of variability of let-7a in normal thyroid tissues is less than 10%. D, Expression of let-7a in rat thyroid cells PC Cl 3 transformed by v-*mos*, v-*raf*, and v-*ras-Ha* oncogenes, compared with the parental nontransformed cell line. E, Let-7a expression in PC Cl 3 after TSH stimulation. The fold change values indicate the relative change in the expression levels between PC Cl 3 cells treated with TSH and PC Cl 3 cells treated with BSA, assuming that the value of the PC Cl 3 cells treated with BSA was equal to 1. Each *bar* represents the mean ± SD from three independent experiments performed in triplicate.

antibodies (Fig. 2D) shows that the typical mesenchymal morphology of WRO cells, characterized by cell scattering, front-rear cell polarization with filopodia-rich front (Fig. 2D, *upper panel*), is substituted by prismatic cell shape and increased cell-cell contacts in WROlet-7a cells (Fig. 2D, *lower panel*). Moreover, actin and tubulin undergo massive reorganization in WROlet-7a cells, giving rise to an evident peripheral actin bordering (Fig. 2D, *lower panel*). Therefore, let-7a restoration confers an epithelial phenotype to the WRO cells.

Then, we examined the effect of let-7a expression on cell adhesion. As shown in Fig. 2E, adhesion of WROlet-7a cells is increased on FN and reduced on VN, compared with WROhU6 cells. Accordingly, WROlet-7a cells show reduced migration on VN, as evidenced by wound-healing experiments (Fig. 2, F and G), indicating that let-7a may negatively affect cell migration.

Let-7a silencing affects cell morphology of normal rat thyroid cells

To further confirm a role of let-7a in thyroid carcinogenesis, we stably inhibited let-7a expression in PC Cl 3 cells by transfecting them with a let-7a-interfering construct (see *Materials and Methods*). As shown in Fig. 3A, the selected cell

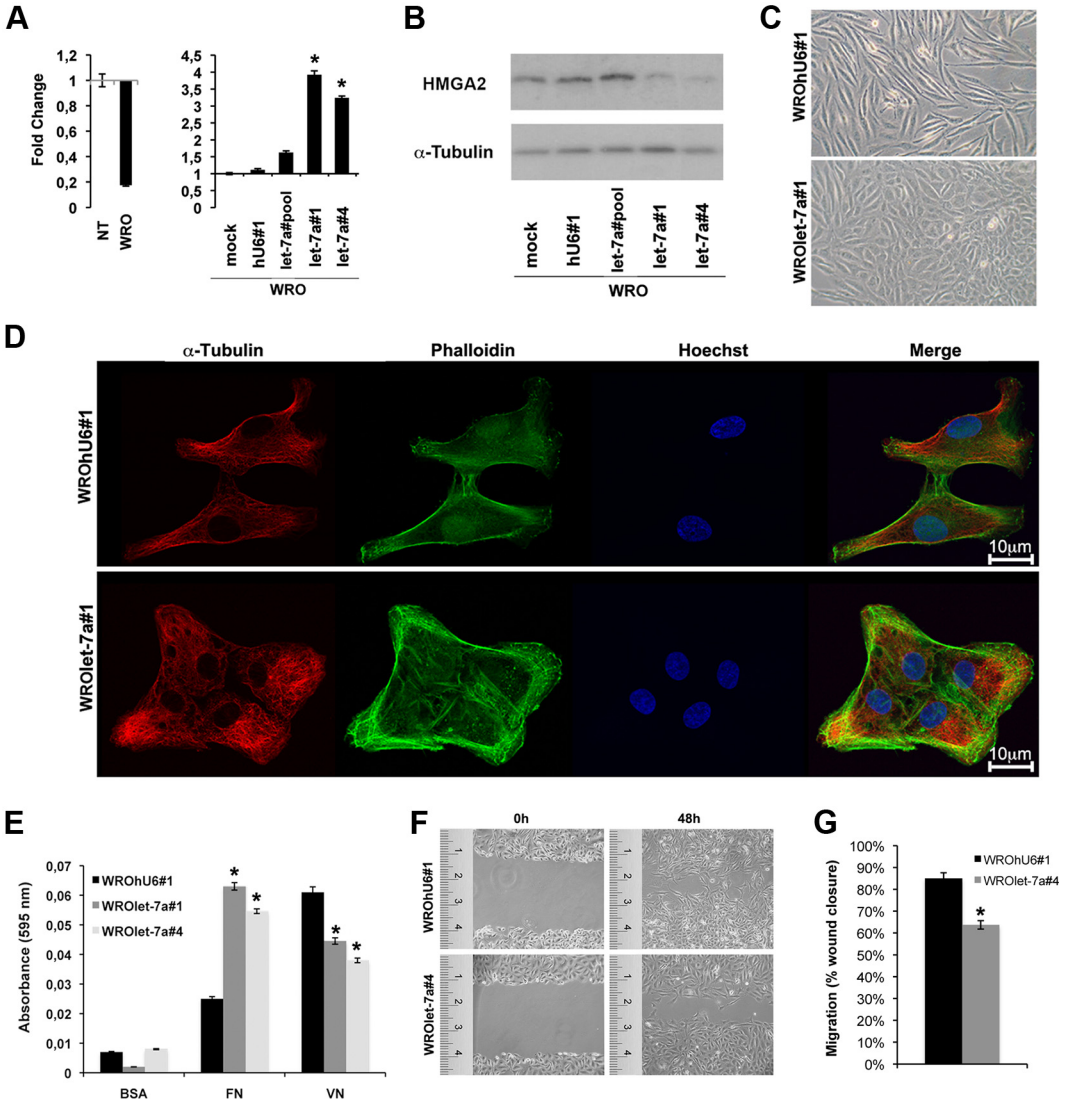

FIG. 2. Effects of let-7a overexpression in WRO cells. A, qRT-PCR analysis of let-7a expression in the human FTC-derived cell line, WRO, compared with normal thyroid (*left panel*) and in WRO cell clones transfected with the empty vector or with the let-7a expressing construct, compared with mock transfected cells (*right panel*). The fold change values indicate the relative change in the expression levels between cell lines and the mean of three normal thyroids (*left panel*) or the mock transfected cells, assuming the latter to be equal to 1. *Asterisks* indicate statistical significance ($P < 0.05$) of differences in let-7a expression between let-7a- *vs.* control vector-transfected clones. B, Western blot analysis for HMGA2 in WRO cell clones stably transfected with the let-7a expressing vector or with the backbone vector. α-tubulin is showed as the loading control. C, Phase contrast micrographs of two representative clones of WROlet-7a and WROhU6 cells. D, Immunofluorescence analysis of WROlet-7a and WROhU6 cells (representative clones) stained with α-tubulin, fluorescein isothiocyanate-conjugated phalloidin, and Hoechst. Magnification, objective 63×/1.40 oil M27. E, Diagram showing adhesion efficiency of WROhU6 and WROlet-7a cell clones on FN and VN. BSA is used as control. *Asterisks* indicate statistical significance ($P < 0.05$) of differences in absorbance in let-7a- *vs.* control vector-transfected cells. F, Scratch assay in two representative clones of WROhU6 and WROlet-7a cells. The wound-induced migration assay in the presence of VN coating was performed in the absence of serum. The extent of cell migration into the wounded area was photographed under phase-contrast microscopy at 0 and 48 h. Magnification, ×100. G, Quantification of the migration assay: the diagram shows data from three separate wound-closure experiments and represents the migration rate, quantified by measuring the distance between the edges of the wound, compared at $t = 0$ to $t = 48$ h and expressed as percentages. *Asterisk* indicates that the difference in migration between let-7a- *vs.* control vector-transfected cells is statistically significant ($P < 0.05$).

clones (PCsilet-7a) show reduced let-7a levels, compared with those transfected with the empty vector (PChU6), and undergo evident morphological changes, including loss of cell-cell contacts, acquisition of irregular shape and formation of pseudopods (Fig. 3B), as well as easier detachment from the substrate after trypsin treatment. Immunofluorescence analyses with phalloidin and anti-α-tubulin antibodies (Fig. 3D) show PChU6 cells assembled in islets with regular epithelial organization, in contrast with PCsilet-7a cells, which lose cell-cell interactions, becoming sparse and "migrating" (Fig. 3C and Supplemental Fig. 1). This phenotype is probably due to E-cadherin delocalization, as evidenced by immunofluorescence performed with anti-E-cadherin antibodies (Supplemental Fig. 1, *left panel*). Although in PChU6, eight-cell-rosettes, uninterrupted circumferential cells, usually surround a single central cell (Fig. 3C, *upper panel*), in

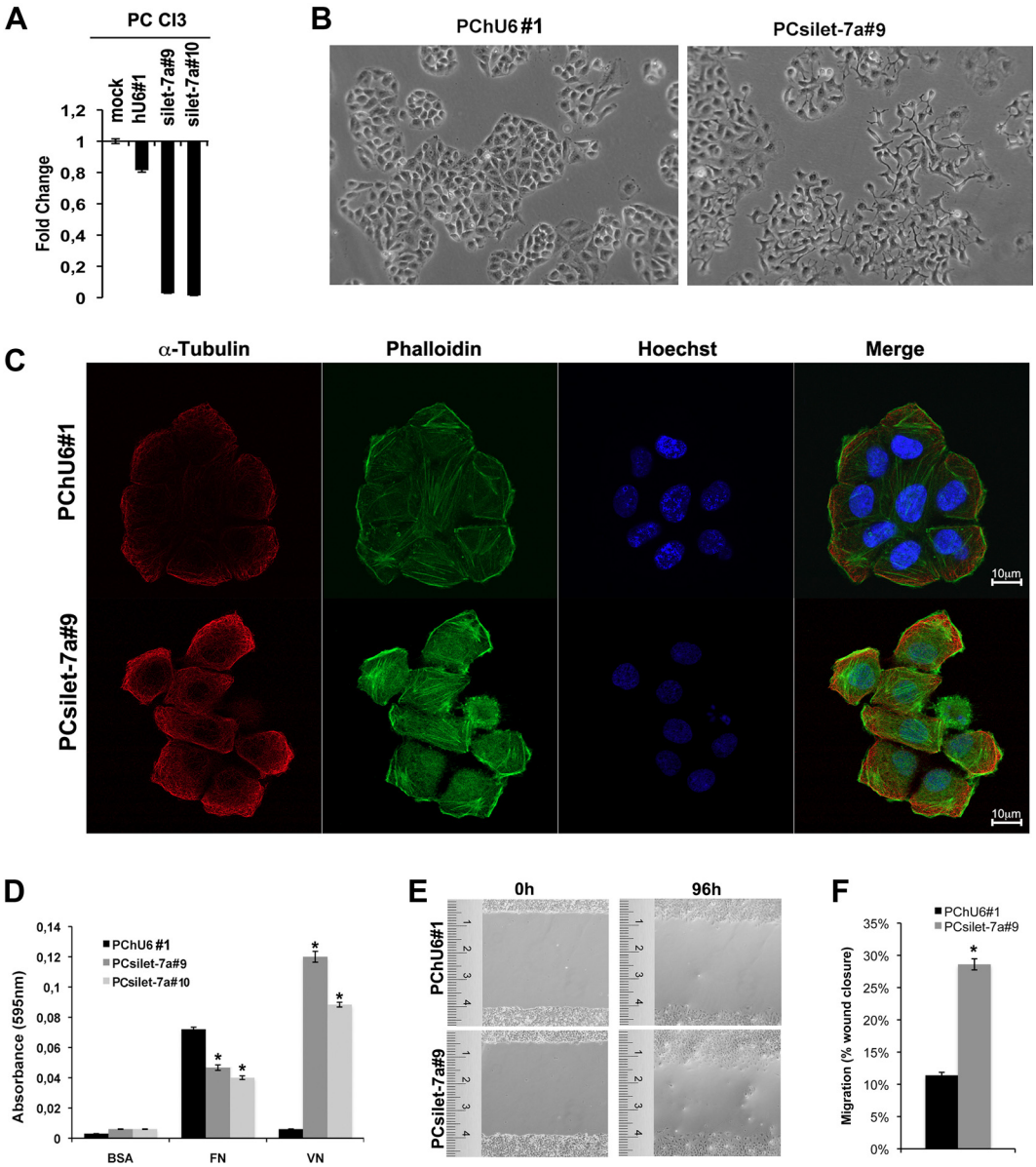

FIG. 3. Effects of let-7a down-regulation in PC Cl 3 cells. A, qRT-PCR analysis of let-7a expression in PC Cl 3 cell clones transfected with the let-7a interfering construct or with the empty vector, compared with mock-transfected cells. B, Phase contrast micrographs of two representative PChU6 and PCsilet-7a cell clones. C, Immunofluorescence analysis of PChU6 and PCsilet-7a cell clones stained with anti α-tubulin antibodies, fluorescein isothiocyanate-conjugated phalloidin, and Hoechst. Magnification, objective 63×/1.40 oil M27. D, Diagram of adhesion ability of PCsilet-7a cell clones compared with that of PChU6 cell clones on FN, VN, or BSA. *Asterisks* indicate statistical significance ($P < 0.05$) of differences in absorbance in let-7a-interfered *vs.* control vector-transfected cells. E, Scratch assay on FN-coated plates. Two representative clones of PChU6 (*upper panels*) and PCsilet-7a cells (*lower panels*) were grown to confluence on FN-coated plates, and a scratch was performed at time 0. Cells were photographed at 0 and 96 h. F, Quantification of the migration assay. The diagram shows data from three separate wound-closure experiments and represents the migration rate, quantified by measuring the distance between the edges of the wound, compared at $t = 0$ to $t = 96$ h and expressed as percentages. *Asterisk* indicates that the difference in migration between let-7a-interfered *vs.* control vector-transfected cells is statistically significant ($P < 0.05$).

PCsilet-7a cells, the rosette organization is completely disassembled (Fig. 3C, *lower panel*). Moreover, tubulin staining evidences loss in cell polarization, being strongly polarized in PChU6, but almost symmetrically distributed around the nucleus in PCsilet-7a cells (Fig. 3C). After staining with phalloidin, PChU6 show cell-cell contacts delimiting cortical actin (Supplemental Fig. 2, *arrowheads*), whereas this feature is lost in PCsilet-7a cells, where actin is predominantly localized in membrane ruffles (Supplemental Fig. 2, *arrows*). Interestingly, this change in actin distribution is suggestive of epithelial-mesenchymal transition (EMT). Furthermore, the nuclei of PCsilet-7a cells show irregular shape and distribution and a certain dishomogeneity after staining with Hoechst, whereas those of the control PChU6 cells appear homogeneous in cell size and uniformly distributed (Fig. 3C and Supplemental Fig. 1).

In adhesion assays performed on VN and FN, the adhesion ability of PCsilet-7a cell clones is reduced on FN and

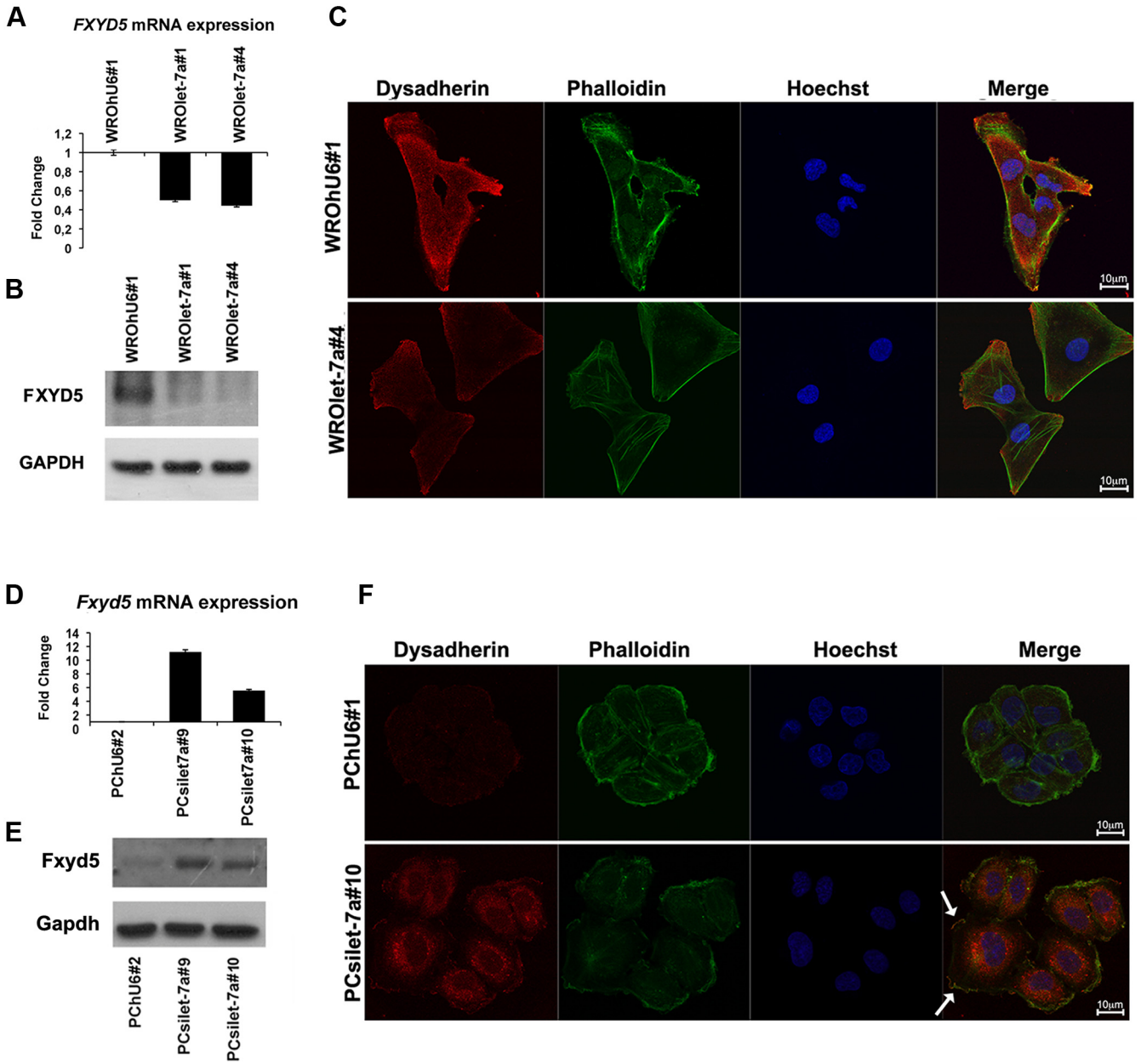

FIG. 4. Dysadherin expression in cells transfected or interfered for let-7a. A, qRT-PCR analysis of *FXYD5* expression in two representative clones of WROlet-7a cells, compared with empty vector-transfected cells. The fold change values indicate the relative change in the expression levels between WROlet-7a cell clones and WROhU6 cells, normalized with glucose-6-phosphate dehydrogenase (G6PD). B, Western blot analysis of dysadherin protein expression in WROlet-7a and WROhU6 extracts. GAPDH has been used as loading control. C, Immunofluorescence analysis of dysadherin and F-actin in WROhU6 and WROlet-7a representative clones. Nuclei were stained with Hoechst (*blue*). Magnification, objective 63×/1.40 oil M27. D, qRT-PCR analysis of *Fxyd5* expression in two representative clones of PCsilet-7a cells, compared with empty vector-transfected cells. The fold change values indicate the relative change in the expression levels between PCsilet-7a cell clones and PChU6 cells, normalized with *G6pd*. E, Western blot analysis of dysadherin protein expression in PChU6 and PCsilet-7a extracts. GAPDH was used as loading control. F, Immunofluorescence analysis of dysadherin and F-actin in PChU6 and PCsilet-7a representative clones. Nuclei were stained with Hoechst (*blue*). Magnification, objective 63×/1.40 oil M27.

increases on VN, compared with PChU6 cells (Fig. 3D). Accordingly, the expression of $\alpha_v\beta_3$ integrin, the VN receptor, analyzed by immunofluorescence, increases in PCsilet-7a cell clones (Supplemental Fig. 3), as evidenced by the merged signal. Moreover, consistent with the reduced adhesion on FN, scratch assays on plates treated with FN (Fig. 3, E and F) and transwell migration assays (Supplemental Fig. 4) in serum-free medium showed an increased migration ability of PCsilet-7a cells on FN compared with PChU6 cells.

Therefore, the modifications observed in the PC Cl 3 cells after silencing of let-7a expression are specular to those observed after restoration of let-7a expression in WRO cells, indicating a key role of let-7a expression in regulating thyroid cell EMT, cell morphology, adhesion, and migration.

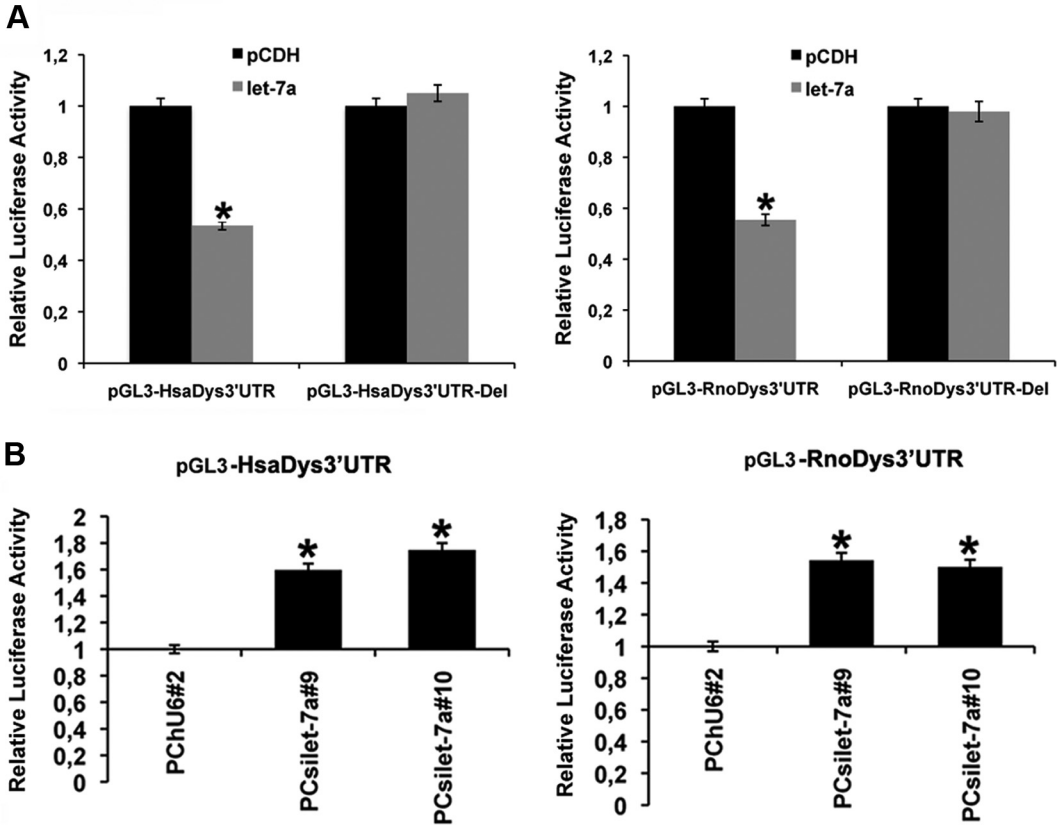

FIG. 5. Let-7a regulates *FXYD5* 3′UTR. A, Relative luciferase activity of human (*left*) and rat (*right*) *FXYD5* 3′UTR in MEG01 cells cotransfected with the pre-let-7a-expressing construct or the empty vector (pCDH). The pGL3-HsaDys3′UTR-Del and pGL3-RnoDys3′UTR-Del constructs carry the *FXYD5* 3′UTR with the deletion in the let-7a target sequence. *Asterisks* indicate statistical significance of difference in luciferase activity between let-7a- and control vector-transfected cells ($P < 0.05$). B, Relative luciferase activity of human (*left*) and rat (*right*) dysadherin 3′UTR in PCsilet-7a, compared with control PChU6 cell clones. *Asterisks* indicate statistical significance of difference in luciferase activity between PChU6 and PCsilet-7a cells ($P < 0.05$). The relative activity of firefly luciferase expression was normalized to a transfection control using Renilla luciferase.

Let-7a targets the *FXYD5* (dysadherin) gene

Because cell-cell adhesion seems to be affected by let-7a expression, we searched for let-7a potential targets involved in cell-cell adhesion and cell migration and altered by thyroid cell transformation. Bioinformatic analysis suggested that one of these candidate targets is the *FXYD5* gene (Supplemental Fig. 5, A and B), which codes for a membrane glycoprotein up-regulated in many tumor types, including thyroid carcinomas (26), and related to increased motility and reduced adhesion (23). To validate the influence of let-7a on *FXYD5*, we evaluated dysadherin mRNA expression in let-7a overexpressing cells: as shown in Fig. 4A, dysadherin expression was reduced in WROlet-7a cell clones compared with WROhU6, indicating a possible effect of let-7a on dysadherin mRNA degradation. In Western blot analysis, the 50-kDa band corresponding to dysadherin was reduced in WROlet-7a cells in comparison with the backbone vector-transfected cells (Fig. 4B). Immunofluorescence analysis, performed with phalloidin and anti-FXYD5 antibodies, confirmed the results obtained by Western blot and showed colocalization of FXYD5 and actin in WROhU6 cells, but not in WROlet-7a cells (Fig. 4C). Accordingly, interfering let-7a expression in PC Cl 3 cells led to increased *Fxyd5* mRNA and protein expression compared with empty vector-transfected cells (Fig. 4, D and E, respectively). Similarly, immunofluorescence analysis demonstrated that the suppression of let-7a expression resulted in dysadherin up-regulation in PCsilet-7a cell clones compared with PChU6 cells (Fig. 4F).

To assess the ability of let-7a to directly regulate dysadherin expression, we performed dual luciferase assays by cotransfecting MEG-01 cells (a human megakaryoblastic leukemia cell line, which expresses very low levels of endogenous let-7) with the pre-let-7a lentiviral vector and the dysadherin-3′ untranslated region (UTR) luciferase reporter construct (either rat or human), carrying a wild-type sequence or deleted in the let-7a target sequence (Supplemental Fig. 5D). Reduction in luciferase activity was observed in MEG01 cells transfected with let-7a compared with empty vector-transfected cells (Fig. 5A). Mutation of the let-7a target sequence makes the reporter construct insensitive to let-7a expression (Fig. 5A), demonstrating that its regulation is dependent on a single tar-

get site located in the *FXYD5* 3′UTR. Accordingly, the luciferase activity of both rat and human dysadherin 3′UTRs was increased in stably interfered PCsilet-7a cell clones in comparison to the control PChU6 (Fig. 5B). Therefore, these results validate a direct posttranscriptional control of dysadherin gene expression by let-7a.

FXYD5 expression inversely correlates with let-7a expression in human thyroid carcinomas

To investigate whether regulation of dysadherin by let-7a occurs also *in vivo* and might have a role in thyroid tumorigenesis, we evaluated dysadherin expression levels in 11 FA and 12 FTC tissues by qRT-PCR analysis. An inverse correlation was found between let-7a and *FXYD5* gene expression at the mRNA level (Fig. 6A). Accordingly, at the protein level, dysadherin was almost not detectable in normal thyroid, whereas FXYD5 was observed in all the FAs and FTCs analyzed (Fig. 6B), although in a couple of FAs (FA no. 4 and FA no. 5), its expression was quite weak; interestingly, these samples showed a very slight decrease in let-7a expression.

Finally, we evaluated Fxyd5 expression also in rat thyroid cells transformed by various oncogenes: dysadherin is present in the transformed cells, where it inversely correlates with let-7a levels, but it is expressed at very low levels in the normal PC Cl 3 cells (Fig. 6C).

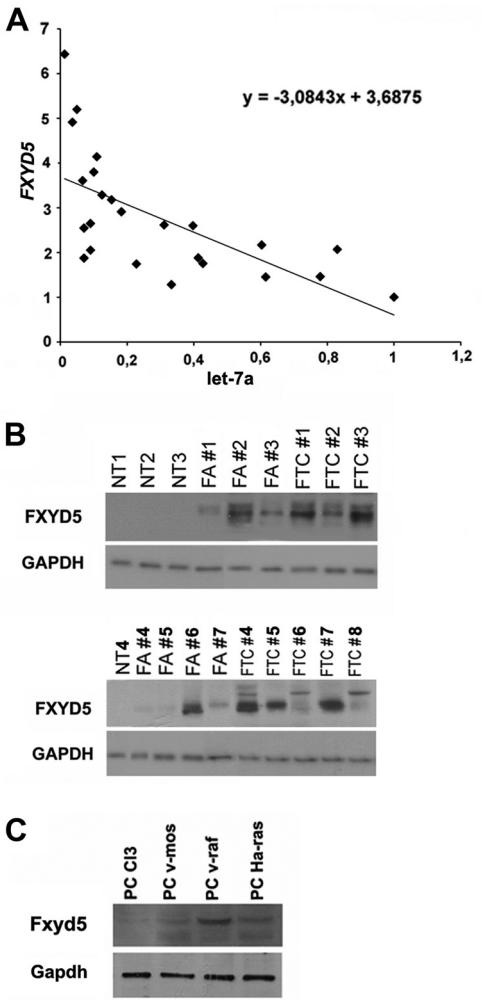

FIG. 6. Inverse correlation between dysadherin and let-7a expression in human thyroid tumors and rat thyroid transformed cells. A, Scatter diagram and trend line showing the inverse correlation between let-7a and *FXYD5* mRNA expression in 11 FAs and 12 FTCs, compared with normal thyroid. The fold change values of let-7a and *FXYD5* obtained by qRT-PCR were plotted on the x- and y-axes, respectively. The pattern of *dots*, sloping from *upper left to lower right*, evidences a negative correlation between let-7a and *FXYD5* gene expression. The equation for the correlation between the two variables is indicated in the diagram. B, Western blot analysis of dysadherin expression in seven FAs and eight FTCs. *Upper and lower panels* show two independent Western blot experiments, performed on different tumor samples and normal thyroids. C, Western blot analysis of dysadherin expression in normal and oncogene-transformed PC Cl 3 cells. GAPDH was used as loading control in B and C.

Discussion

In this study, we first analyzed the miRNA expression profile of 10 FAs *vs.* 10 normal thyroid tissues. Because let-7 was one of the miRNAs constantly down-regulated in thyroid adenomas with the highest fold change, we concentrated our studies on this miRNA. This choice was also supported by several data in literature showing let-7a down-regulation in several cancer types and that the reduction in its levels induces tumorigenicity in various cell lines (27). Then, we have shown that let-7a is also down-regulated in FTCs, with an average fold change that is significantly higher in comparison with that observed in FAs. Interestingly, let-7a is down-regulated also in rat thyroid cells transformed by viral oncogenes.

Let-7 down-regulation has been previously described in PTCs (28). It has also been shown that let-7f induction in TPC-1 cells, a human PTC cell line that harbors the RET/PTC1 oncogene, causes a marked reduction in cell proliferation and induces expression of molecular markers of thyroid differentiation, suggesting that let-7 miRNA plays a role in thyroid carcinogenesis (28).

To define the role of let-7a down-regulation in cell transformation and tumor progression, let-7a expression was restored in WRO cell line, deriving from a FTC, and blocked in the normal thyroid cell line PC Cl 3. In both cases, the alterations in let-7a expression induced changes at the cell surface, leading to modification in cell morphology, adhesion, and migration. Indeed, the let-7a-overexpressing WRO cells shifted their morphology from a fibroblastoid shape to an epithelial one, showed an increased adhesion on FN and reduced adhesion on VN compared with WROhU6 cells. These changes were associated with a reduced migratory ability, as assessed by migration and invasion assays. Conversely, the PC Cl 3

cells interfered for let-7a expression acquired a fibroblast-like shape with decreased adhesion to the plate and increased motility. Therefore, our results would suggest a new role for let-7 in migration and adhesion that may have implications in cancerogenesis and tissue morphogenesis. Based on our results, this role seems to be mediated at the molecular level by the pleiotropic effect that let-7 exerts on adhesion molecules, such as integrins, dysadherin, and E-cadherin.

These data are consistent with previous studies demonstrating the ability of let-7a to regulate β3 integrin expression in melanoma (29) and the role of let-7f in inhibiting cell migration and invasion in gastric cancer cells by directly targeting the tumor metastasis-associated gene MYH9 (30). Moreover, Shell *et al.* (31) have proposed let-7 as a good candidate to define the "epithelial" gene signature. More precisely, let-7 was found to be a marker for differentiating human tumor cell lines with an epithelial gene signature (supercluster 2 or SC2) from those with a mesenchymal signature (SC1) more reliable than classical markers such as E-cadherin, vimentin, and Snail. Our data, other than confirming let-7a as a marker of EMT, also propose a direct role of let-7a in inducing epithelial transition.

We have identified the *FXYD5* gene as a novel target of let-7a. FXYD5 protein is a single-span membrane glycoprotein, belonging to a family of transmembrane proteins, characterized by 35-amino acid signature sequence (32). Dysadherin is up-regulated in v-*ras*, v-*src*- and *neu*-transformed NIH3T3 cells (33) and overexpressed in several human cancers (23, 34, 35). It specifically interacts with the Na^+-K^+-ATPase, modulating its kinetic properties (36), and functionally inactivates or delocalizes E-cadherin (34, 35).

We show that the restoration of let-7a expression reduces FXYD5 levels, whereas let-7a depletion increases them. The inverse correlation found between let-7a expression and *FXYD5* mRNA levels in WROlet-7a and PCsilet-7a suggests that let-7a regulates FXYD5 protein expression also by affecting dysadherin mRNA degradation. These results are in agreement with data from Guo *et al.* (37), demonstrating that changes in mRNA levels closely reflect the impact of miRNAs on gene expression and that destabilization of target mRNAs may be a reason for reduced protein output. Moreover, we demonstrate that let-7a directly regulates *FXYD5* mRNA expression because it negatively regulates the expression of an *FXYD5* 3′UTR-based reporter construct.

Interestingly, we have found a certain inverse correlation between let-7a expression and FXYD5 protein levels in FAs and FTCs, suggesting a role of let-7a in regulating FXYD5 protein levels also *in vivo*. Similar correlation has also been observed in rat thyroid transformed cells.

The ability of let-7a to target the *FXYD5* gene likely accounts for most of the phenotypic modifications observed in the WROlet-7a and PCsilet-7a cells with respect to the control cells. Indeed, dysadherin down-regulation in pancreatic cells is associated with an enlarged, flattened, and more adherent-looking morphology (23), which resembles the phenotype of WROlet-7a cells. Finally, dysadherin is associated with poor prognosis, occurrence of secondary undifferentiated carcinomas, size of primary tumor, and metastasis to lymph nodes, and it is also inversely related with E-cadherin function in human thyroid carcinomas (26).

Recently, dysadherin has been shown to confer stem-like properties to hepatocellular carcinoma cells (38). Because let-7a down-regulation has also been considered a "stemness"-inducing factor (39), we could envisage the hypothesis that the loss of let-7 might have a role in cell stemness induction by also regulating dysadherin protein levels.

In conclusion, taken together, the results shown here indicate a critical role of let-7a down-regulation in thyroid carcinogenesis of follicular histotype by modifying cell morphology, adhesion, and migration of thyroid cells likely through its ability to regulate dysadherin protein levels.

Acknowledgments

We thank Dr. Setsuo Hirohashi (National Cancer Center Research Institute, Tokyo 104-0045, Japan) for providing us with the antihuman FXYD5 monoclonal antibody.

Address all correspondence and requests for reprints to: Alfredo Fusco, Istituto di Endocrinologia ed Oncologia Sperimentale del Consiglio Nazionale delle Ricerche, Via Pansini 5, 80131 Napoli, Italy. E-mail: alfusco@unina.it.

This work was supported by Associazione Italiana Ricerca sul Cancro (IG5346) and Ministero dell'Università e della Ricerca.

Confocal microscopy was performed at DIM facility CEINGE Biotecnologie Avanzate.

Disclosure Summary: The authors have nothing to disclose.

References

1. **Kondo T, Ezzat S, Asa SL** 2006 Pathogenetic mechanisms in thyroid follicular-cell neoplasia. Nat Rev Cancer 6:292–306
2. **Sobrinho-Simões M, Eloy C, Magalhães J, Lobo C, Amaro T** 2011 Follicular thyroid carcinoma. Mod Pathol 24(Suppl 2):S10–S18
3. **Palos-Paz F, Perez-Guerra O, Cameselle-Teijeiro J, Rueda-Chimeno C, Barreiro-Morandeira F, Lado-Abeal J, Araujo Vilar D, Argueso R, Barca O, Botana M, Cabezas-Agrícola JM, Catalina P, Dominguez Gerpe L, Fernandez T, Mato A, Nuño A, Penin M, Victoria B**

2008 Prevalence of mutations in TSHR, GNAS, PRKAR1A and RAS genes in a large series of toxic thyroid adenomas from Galicia, an iodine-deficient area in NW Spain. Eur J Endocrinol 159:623–631

4. **Kroll TG, Sarraf P, Pecciarini L, Chen CJ, Mueller E, Spiegelman BM, Fletcher JA** 2000 PAX8-PPARγ1 fusion oncogene in human thyroid carcinoma. Science 289:1357–1360
5. **Gudmundsson J, Sulem P, Gudbjartsson DF, Jonasson JG, Sigurdsson A, Bergthorsson JT, He H, Blondal T, Geller F, Jakobsdottir M, Magnusdottir DN, Matthiasdottir S, Stacey SN, Skarphedinsson OB, Helgadottir H, Li W, Nagy R, Aguillo E, Faure E, Prats E, Saez B, Martinez M, Eyjolfsson GI, Bjornsdottir US, Holm H, Kristjansson K, Frigge ML, Kristvinsson H, Gulcher JR, Jonsson T, Rafnar T, Hjartarsson H, Mayordomo JI, de la Chapelle A, Hrafnkelsson J, Thorsteinsdottir U, Kong A, Stefansson K** 2009 Common variants on 9q22.33 and 14q13.3 predispose to thyroid cancer in European populations. Nat Genet 41:460–464
6. **Garzon R, Calin GA, Croce CM** 2009 MicroRNAs in cancer. Annu Rev Med 60:167–179
7. **Pallante P, Visone R, Ferracin M, Ferraro A, Berlingieri MT, Troncone G, Chiappetta G, Liu CG, Santoro M, Negrini M, Croce CM, Fusco A** 2006 MicroRNA deregulation in human thyroid papillary carcinomas. Endocr Relat Cancer 13:497–508
8. **Visone R, Pallante P, Vecchione A, Cirombella R, Ferracin M, Ferraro A, Volinia S, Coluzzi S, Leone V, Borbone E, Liu CG, Petrocca F, Troncone G, Calin GA, Scarpa A, Colato C, Tallini G, Santoro M, Croce CM, Fusco A** 2007 Specific microRNAs are downregulated in human thyroid anaplastic carcinomas. Oncogene 26:7590–7595
9. **Ruby JG, Jan C, Player C, Axtell MJ, Lee W, Nusbaum C, Ge H, Bartel DP** 2006 Large-scale sequencing reveals 21U-RNAs and additional microRNAs and endogenous siRNAs in *C. elegans*. Cell 127:1193–1207
10. **Yanaihara N, Caplen N, Bowman E, Seike M, Kumamoto K, Yi M, Stephens RM, Okamoto A, Yokota J, Tanaka T, Calin GA, Liu CG, Croce CM, Harris CC** 2006 Unique microRNA molecular profiles in lung cancer diagnosis and prognosis. Cancer Cell 9:189–198
11. **Yu F, Yao H, Zhu P, Zhang X, Pan Q, Gong C, Huang Y, Hu X, Su F, Lieberman J, Song E** 2007 Let-7 regulates self renewal and tumorigenicity of breast cancer cells. Cell 131:1109–1123
12. **Zhang HH, Wang XJ, Li GX, Yang E, Yang NM** 2007 Detection of let-7a microRNA by real-time PCR in gastric carcinoma. World J Gastroenterol 13:2883–2888
13. **Kumar MS, Erkeland SJ, Pester RE, Chen CY, Ebert MS, Sharp PA, Jacks T** 2008 Suppression of non-small cell lung tumor development by the let-7 microRNA family. Proc Natl Acad Sci USA 105:3903–3908
14. **Johnson SM, Grosshans H, Shingara J, Byrom M, Jarvis R, Cheng A, Labourier E, Reinert KL, Brown D, Slack FJ** 2005 RAS is regulated by the let-7 microRNA family. Cell 120:635–647
15. **Lee YS, Dutta A** 2007 The tumor suppressor microRNA let-7 represses the HMGA2 oncogene. Genes Dev 21:1025–1030
16. **Chang TC, Yu D, Lee YS, Wentzel EA, Arking DE, West KM, Dang CV, Thomas-Tikhonenko A, Mendell JT** 2008 Widespread microRNA repression by Myc contributes to tumorigenesis. Nat Genet 40:43–50
17. **Johnson CD, Esquela-Kerscher A, Stefani G, Byrom M, Kelnar K, Ovcharenko D, Wilson M, Wang X, Shelton J, Shingara J, Chin L, Brown D, Slack FJ** 2007 The let-7 microRNA represses cell proliferation pathways in human cells. Cancer Res 67:7713–7722
18. **Colamaio M, Borbone E, Russo L, Bianco M, Federico A, Califano D, Chiappetta G, Pallante P, Troncone G, Battista S, Fusco A** 2011 MiR-191 down-regulation plays a role in thyroid follicular tumors through CDK6 targeting. J Clin Endocrinol Metab 96:E1915–E1924
19. **Estour B, Van Herle AJ, Juillard GJ, Totanes TL, Sparkes RS, Giuliano AE, Klandorf H** 1989 Characterization of a human follicular thyroid carcinoma cell line (UCLA RO 82 W-1). Virchows Arch B Cell Pathol Incl Mol Pathol 57:167–174
20. **Fusco A, Berlingieri MT, Di Fiore PP, Portella G, Grieco M, Vecchio G** 1987 One- and two-step transformations of rat thyroid epithelial cells by retroviral oncogenes. Mol Cell Biol 7:3365–3370
21. **Pallante P, Berlingieri MT, Troncone G, Kruhoffer M, Orntoft TF, Viglietto G, Caleo A, Migliaccio I, Decaussin-Petrucci M, Santoro M, Palombini L, Fusco A** 2005 UbcH10 overexpression may represent a marker of anaplastic thyroid carcinomas. Br J Cancer 93:464–471
22. **Di Agostino S, Fedele M, Chieffi P, Fusco A, Rossi P, Geremia R, Sette C** 2004 Phosphorylation of high-mobility group protein A2 by Nek2 kinase during the first meiotic division in mouse spermatocytes. Mol Biol Cell 15:1224–1232
23. **Shimamura T, Yasuda J, Ino Y, Gotoh M, Tsuchiya A, Nakajima A, Sakamoto M, Kanai Y, Hirohashi S** 2004 Dysadherin expression facilitates cell motility and metastatic potential of human pancreatic cancer cells. Cancer Res 64:6989–6995
24. **Naik MU, Naik UP** 2006 Junctional adhesion molecule-A-induced endothelial cell migration on vitronectin is integrin α v β 3 specific. J Cell Sci 119:490–499
25. **Liu CG, Calin GA, Meloon B, Gamliel N, Sevignani C, Ferracin M, Dumitru CD, Shimizu M, Zupo S, Dono M, Alder H, Bullrich F, Negrini M, Croce CM** 2004 An oligonucleotide microchip for genome-wide microRNA profiling in human and mouse tissues. Proc Natl Acad Sci USA 101:9740–9744
26. **Sato H, Ino Y, Miura A, Abe Y, Sakai H, Ito K, Hirohashi S** 2003 Dysadherin: expression and clinical significance in thyroid carcinoma. J Clin Endocrinol Metab 88:4407–4412
27. **Kumar MS, Lu J, Mercer KL, Golub TR, Jacks T** 2007 Impaired microRNA processing enhances cellular transformation and tumorigenesis. Nat Genet 39:673–677
28. **Ricarte-Filho JC, Fuziwara CS, Yamashita AS, Rezende E, da-Silva MJ, Kimura ET** 2009 Effects of let-7 microRNA on cell growth and differentiation of papillary thyroid cancer. Transl Oncol 2:236–241
29. **Müller DW, Bosserhoff AK** 2008 Integrin β 3 expression is regulated by let-7a miRNA in malignant melanoma. Oncogene 27:6698–6706
30. **Liang S, He L, Zhao X, Miao Y, Gu Y, Guo C, Xue Z, Dou W, Hu F, Wu K, Nie Y, Fan D** 2011 MicroRNA let-7f inhibits tumor invasion and metastasis by targeting MYH9 in human gastric cancer. PLoS One 6:e18409
31. **Shell S, Park SM, Radjabi AR, Schickel R, Kistner EO, Jewell DA, Feig C, Lengyel E, Peter ME** 2007 Let-7 expression defines two differentiation stages of cancer. Proc Natl Acad Sci USA 104:11400–11405
32. **Sweadner KJ, Rael E** 2000 The FXYD gene family of small ion transport regulators or channels: cDNA sequence, protein signature sequence, and expression. Genomics 68:41–56
33. **Fu X, Kamps MP** 1997 E2a-Pbx1 induces aberrant expression of tissue-specific and developmentally regulated genes when expressed in NIH 3T3 fibroblasts. Mol Cell Biol 17:1503–1512
34. **Ino Y, Gotoh M, Sakamoto M, Tsukagoshi K, Hirohashi S** 2002 Dysadherin, a cancer-associated cell membrane glycoprotein, down-regulates E-cadherin and promotes metastasis. Proc Natl Acad Sci USA 99:365–370
35. **Nam JS, Hirohashi S, Wakefield LM** 2007 Dysadherin: a new player in cancer progression. Cancer Lett 255:161–169
36. **Lubarski I, Karlish SJ, Garty H** 2007 Structural and functional interactions between FXYD5 and the Na+-K+-ATPase. Am J Physiol Renal Physiol 293:F1818–F1826
37. **Guo H, Ingolia NT, Weissman JS, Bartel DP** 2010 Mammalian microRNAs predominantly act to decrease target mRNA levels. Nature 466:835–840
38. **Park JR, Kim RJ, Lee YK, Kim SR, Roh KJ, Oh SH, Kong G, Kang KS, Nam JS** 2011 Dysadherin can enhance tumorigenesis by conferring properties of stem-like cells to hepatocellular carcinoma cells. J Hepatol 54:122–131
39. **Dröge P, Davey CA** 2008 Do cells let-7 determine stemness? Cell Stem Cell 2:8–9